ELSEVIER

Chemical Engineering Journal 132 (2007) 85–95

Chemical Engineering Journal

www.elsevier.com/locate/cej

Methane oxidative conversion pathways in a dielectric barrier discharge reactor—Investigation of gas phase mechanism

S.A. Nair *, Tomohiro Nozaki, Ken Okazaki

Department of Mechanical & Control Engineering, Tokyo Institute of Technology, 2-12-1 O-Okayama, Meguro-ku, 152-8552 Tokyo, Japan

Received 6 June 2006; received in revised form 24 December 2006; accepted 17 January 2007

Abstract

Non-thermal plasma, over the past few years, is being investigated for methane conversion. In order to improve the efficiency, combined plasma and catalyst is being explored to exploit possible synergetic effects. The present paper investigates plasma assisted methane conversion in gas phase by partial oxidation at low energy density (80–200 kJ/mol CH_4) and low reactor temperatures (130–140 °C). Although non-thermal plasma has the inherent advantage of initiating reactions, a disadvantage is the unfavorable selectivity to the desired product. The investigation attempts to identify the plasma initiated chemical reaction pathways by combining experiments and kinetic modeling. Sensitivity analysis indicates reaction intermediates leading to formation of oxygenates as an alternative oxidation pathway at the investigated temperatures ($T < 200$ °C). The selectivity for synthesis gas formation could be increased by partial oxidation at higher CH_4/O_2 ratios. Combined partial oxidation and steam reforming was as well investigated in order to increase H_2 concentration. Isotopes were used in order to identify reaction pathways for the case of steam reforming experiments. However, experiments at lower energy density indicate negligible steam conversion. At lower temperatures, the input plasma energy is primarily used for CH_4/O_2 conversion.

Keywords: Non-thermal plasma; Partial oxidation; Dielectric barrier discharges; Plasma chemistry; Kinetic modeling

1. Introduction

Methane steam reforming is commercially used as a viable process for synthesis gas production. However, partial oxidation has always been a desired process due to its exothermic nature. But in order to exploit oxidative conversion, the following technical problems need to be overcome [1]:

(a) High temperatures (>800 K) are needed for activation of methane molecule. This calls for very stable materials, if a catalytic reactor is used (which is often done for the sake of selectivity).
(b) At these extreme conditions, carbon formation reactions are favored (973 K < T < 1273 K), which leads to coke deposition and blockage of active sites coupled with plugging of the reactor, hindering regular operation.

Non-thermal plasma, due to its ability to create reactive species, can be an alternative method for excitation of methane molecule, either by direct electron impact dissociation or by indirect radical reactions. This principle has been used for removal of compounds (pollution control) with varying degree of success. Investigations into processes such as plasma induced NOx and SOx removal, VOC removal from air or air like mixtures, at room temperature to 100 °C, have indicated the removal mechanism to be initiated by formation of O species [2]. Likewise, studies focusing on the removal of polyaromatic hydrocarbons from fuel gas mixtures, at temperature ranging from 200 to 500 °C, have indicated primary mechanism to be CO_2 dissociation [3,4]. Thus, due to its inherent ability to create reactive species, non-thermal plasma can be utilized to initiate or sustain reactions at lower operating temperatures. Similar approach is intended for C_1 partial oxidation process. In this context, various reactor configurations have been studied for this application. A point to plate configuration with a con-current flow in an ac discharge reactor has indicated CH_4 conversion in the range of 10–20% for a CH_4/O_2 ratio of 3–5 at energy consumption of 10 eV/(molecule of CH_4) (960 kJ/mol of CH_4) [5]. The H_2/CO ratio was reported to be in the range of 2–3, with a selectivity of

* Corresponding author. Present address: Aditya Birla Science and Technology Company Ltd., Aditya Birla Group, Plot no. 1 & 1-A1, MIDC Taloja, Navi Mumbai 410208, Maharashtra, India. Tel.: +91 22 2740 3147.
E-mail address: Nair.s.a@gmail.com (S.A. Nair).

1385-8947/$ – see front matter © 2007 Elsevier B.V. All rights reserved.
doi:10.1016/j.cej.2007.01.022

20–30% for C_2 products at room temperature. Combined plasma catalyst reactor can be an alternative pathway to improve selectivity. However, in order to choose an appropriate catalyst or design a catalyst, essential information is the knowledge of gas phase reaction, especially for the case of non-thermal plasma induced processes. For the case of plasma catalytic CH_4 partial oxidation process, dielectric barrier discharge (DBD) reactors have been used in the temperature range from 200 to 400 °C at energy density in the order of 800–1000 kJ/mol CH_4 [6]. Results reported over α-Al_2O_3 as a bed material indicate H_2 selectivity to be in the order of 20–30% at the temperatures investigated. In presence of a commercial Ni/γAl_2O_3 catalyst, the H_2 selectivity was higher (60%) at temperatures higher than 400 °C.

In spite of such investigations, there is still a lack of information about the basic chemical mechanisms, since the main focus is on increasing CH_4 conversion. A consequence of the ongoing "plasma CH_4 conversion race" is the high energy used in the experiments. This results in conversion of input electrical energy into thermal heat or joule heating. The observed conversion is then a result of thermal process, masking the plasma process. From energy efficiency point of view, non-thermal plasma induced radical initiated process would be beneficial than utilizing non-thermal plasma as a heat source. The present investigation thus attempts to study methane conversion at low energy levels in DBD reactors to elucidate the chemical reaction pathways. Low temperatures are used to focus on plasma process. As a first step, only gas phase processing is investigated. Combined partial oxidation and steam reforming is studied as an alternative way to increase H_2 production by dissociation of water molecules or by induced radical dissociation process. To summarize, we attempt to focus on:

(a) reaction pathways for product formation from plasma assisted partial oxidation process;
(b) reactions influencing desired product formation;
(c) influence of non-thermal plasma for the case of combined steam and partial oxidation process.

2. Experimental set-up

The experiments are carried out in a DBD reactor (glass tube) with an inner diameter of 1 cm and length of 7 cm, thus a total reactor volume of 5.5 cm^3. The high voltage electrode consists of SS-304 rod with a diameter of 0.1 cm, energized by a high voltage amplifier (TREK). A steel foil wrapped around the tube serves as a ground electrode. The entire set-up was placed inside an oven to have uniform temperature (T = 130 °C). CH_4 and O_2 were the principle reactants for the experiments, fed at varying ratios. In order to establish mass balance, CH_4 was fed with 10% N_2. The reactor was energized by an ac high voltage 12–13 kV at a frequency of 250 Hz, with a power equivalent of 3 W. The input power was limited to these values so as not to increase temperature of the packed bed by way of plasma heating. At a power input of 3 W, the resulting temperature increase at the outer electrode was in the order of 10 °C. Thus, on account of low energy density, methane conversions were low (1–2%). The product composition was measured by a GC equipped with a thermal conductivity detector (TCD) (H_2, CH_4 measurements), and a FID (for CO and hydrocarbon measurements) (Fig. 1).

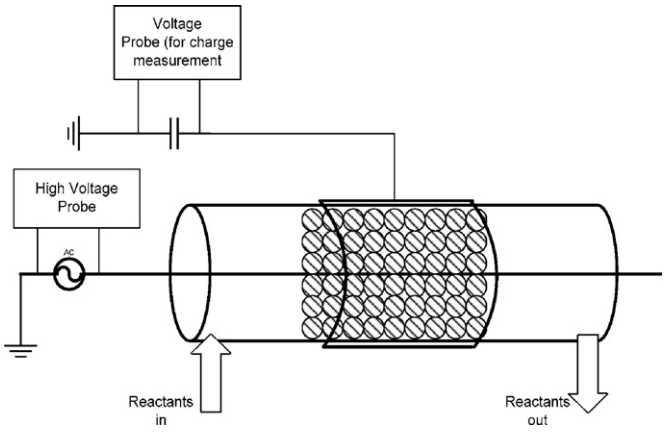

Fig. 1. Experimental set-up.

For the case of combined partial oxidation and steam reforming, D_2O (heavy water) was used to track steam conversion. Steam was injected into the reactor by means of a constant feeding pump at a rate of 4 ml/h. A QMS (quadrapole mass spectrometer, Balzers) was used to distinguish the species H_2, HD, D_2 formed during the conversion process. Product composition is reported in terms of the moles of product formed per mole of CH_4 converted.

Product selectivity = moles of product formed/moles of C detected at the output.

3. Results

3.1. Experimental investigation

Plasma assisted partial oxidation was performed in gas phase as well as different bed materials in order to investigate the effect of packing material in the discharge. α-Al_2O_3 and Ni/γ-Al_2O_3 was used as a bed material/catalyst in order to simultaneously investigate the effect of a catalyst. Experiments were carried out at CH_4/O_2 ratio of 2 (CH_4 = 44 sccm, O_2 = 21 sccm) at temperatures of 130 °C (electrode temperature = 138 °C) and energy density of 80–100 kJ/mol CH_4 (total energy = 800 J/l (total gas flow rate)). Fig. 2(a) indicates the product selectivity observed over different packing materials. In all the cases, the observed selectivity for C_2 production was rather low (<2%). H_2 selectivity is in the order of 30 %, while CO/CO_2 ratio is about 2.

α-Al_2O_3, by itself, does not exhibit any catalytic activity at the experimental conditions (T = 130–150 °C) for methane conversion. Furthermore, in presence of plasma, it has been reported that the observed conversion is same as the case for an empty DBD [6], which was also seen in our experiments as well. The observed product distribution remained largely unchanged even at higher energy densities for the case of gas phase process. At higher temperatures (T > 300–400 °C), the nature of bed material seems to have an influence on the product composition [6]. In order to determine, if the H_2 oxidation reaction is a surface

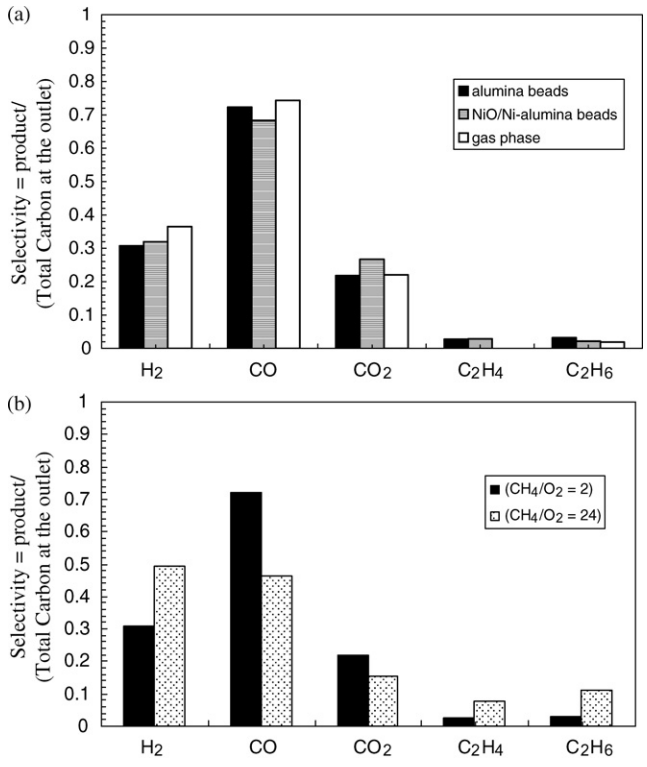

Fig. 2. (a) Experiments over different bed materials and (b) experiments at different CH_4/O_2 ratio.

reaction or a gas phase reaction at the investigated temperatures, conversion over Ni/γ-Al_2O_3 was studied. It is known that Ni has a high reforming activity and therefore we can expect higher H_2 production if surface reaction do play a role. However, the activation temperature for such a catalyst composition is high (>400 °C), hence no significant difference in reaction pathways is observed. Nevertheless, a DBD discharge with the present configuration does not seem to change/affect the activity of a catalyst. Further, as can be seen from experimental results, the catalytic surfaces do not participate in the reaction pathway. This may be because of the low temperatures (less than the temperature needed for the activation of the catalytic surface, such as Ni) used for the experimental study. In other words, at the experimental conditions, the product distribution is only influenced by plasma initiated process. Fig. 2(b) indicates the product distribution as observed for the case of partial oxidation in lean O_2 mixture ($CH_4/O_2 = 24$). Apart from the indicated product distribution, C_3 formation was as well observed. From the results in Fig. 2, it can be observed that the H_2/CO formation seems to be limited by its relative oxidation rates. A logical interpretation would be the limitation imposed by the competitive reaction rates for H_2 consumption and formation. In other words, the H_2 selectivity primarily seems to be dictated by the fast H_2–O_2 reaction to form H_2O. Based on the above analysis, a decrease in O radical concentration would therefore limit the excessive H oxidation and increase selectivity towards H_2 production. Accordingly, experiments at higher CH_4/O_2 ratios favored H_2 formation as seen in Fig. 2(b). Thus, controlling gas phase interactions is one possible alternative to increase or change product distribution. Similar observations have been made other groups that the product distribution from plasma assisted partial oxidation process is primarily a result of gas phase reactions [6].

3.2. Kinetic modeling

In order to further study gas phase process and to have more insight into the chemical mechanism, a simple kinetic model has proven to be a useful technique [3,4,7–9]. Non-thermal plasma chemical process involves active generation of electrons, metastables and ions and their induced chemical reactions. All the physical processes contribute to generation of radicals. To depict an actual process, one needs to have a "perfect" discharge model to describe the distribution of the species produced in both the axial and radial directions. Unfortunately, this is far from reality. Hence, in this paper, a fitting parameter is used to evaluate the amount of radicals necessary for the conversion process as observed experimentally. In the present numerical calculation, radical production is incorporated in the rate constant of the process [7]. Therefore, both phases in the reactor, viz. the plasma phase as well as the bulk gas phase are well mixed; hence, the model can be termed as a pseudo-homogenous model. Similar approaches have been done in past works by other researchers and useful information related to the discharge chemistry has been obtained [3,4,7–9].

The numerical calculation is done with the following assumptions:

(1) radicals produced are well mixed with reactants;
(2) radicals once produced are uniformly distributed within the whole volume, i.e. a zero-dimensional model;
(3) chemistry of the process is solely described by radical behavior;
(4) initial radical production is directly proportional to the related bulk gas composition;
(5) thermal decomposition at the conditions of the experiment (T = 130–200 °C) is negligible.

Similar to decomposition mechanism described elsewhere [8,9], the initial plasma reaction is represented by the following four reactions:

$$e + CH_4 \rightarrow CH_3 + H + e; \qquad e + CH_4 \rightarrow CH_2 + H_2 + e;$$

$$e + CH_4 \rightarrow CH + 3H + e; \qquad e + O_2 \rightarrow 2O + e$$

A total of 180 reactions with 29 species are used to describe the plasma assisted CH_4 partial oxidation at the conditions of the experiment (T = 130–200 °C) (Appendix A).

Molecular species: H_2, O_2, H_2O, H_2O_2, CH_4, CO, CO_2, CH_3OH, CH_2O, C_2H_2, C_2H_4, C_2H_6, C_3H_8.

Radical species: H, O, OH, HO_2, CH, CH_2, CH_3, HCO, CH_2OH, CH_3O, C_2H, C_2H_3, C_2H_5, HCCO, C_3H_7, CH_2CO.

The oxidation scheme represented in the numerical calculation is indicated in Fig. 3. As observed from experimental results, C_3 formation was included in the calculation process. Solid formation reactions, and formation of C_2 and C_3 oxygenates were not considered in the present case as was observed

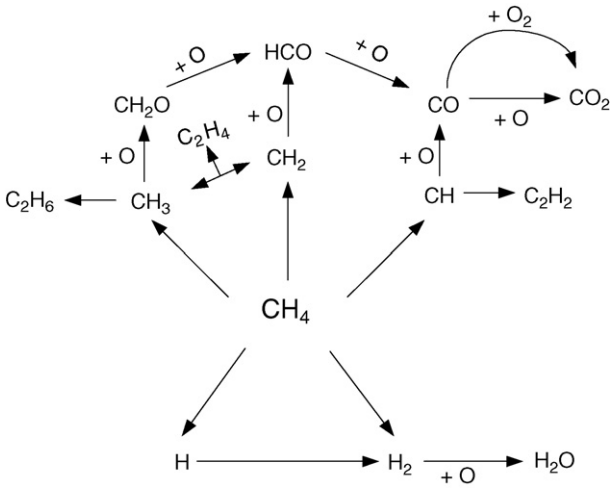

Fig. 3. Reaction scheme for calculation.

in the experiments as well. CO termination to CO_2 was done by way of radical reactions as well as by additional oxidation pathway which occurs at the wall or in the high temperature zones in the vicinity of a micro discharge. The aim of the calculation is mainly to identify the reaction which can influence the final product selectivity and hence incorporate an appropriate catalytic surface.

The general reaction scheme and the format of the mass conservation equations are:

$$A \rightarrow R; \qquad R + X \rightarrow \text{Products}$$

The initial radical production and its consumption can be expressed as:

$$\frac{\mathrm{d}[R_i]}{\mathrm{d}t} = G_\mathrm{R} \cdot E - \sum_j k_{ij} \cdot [R_i] \cdot [X_j] \tag{1}$$

and otherwise the mass conservation of the species is expressed as:

$$\frac{\mathrm{d}[X_i]}{\mathrm{d}t} = \sum_j k_{ji} \cdot [X_i] \cdot [X_j] \tag{2}$$

where G_R is the radical production per Joule per m^3 (mol/(J m^3)): $K_\mathrm{R} \cdot \lambda_\mathrm{R} \cdot [M]$, K_R the dissociation constant (fitting parameter) (J^{-1}), M the bulk gas concentration (mol/m^3), λ_R the gas volume fraction, E the energy (W), k the reaction rate constant (s^{-1}), $[X_i]$, $[R_i]$ the species concentration (mol/m^3) and $[A]$ is the gas component such as H_2, CO_2, H_2O.

According to the above hypothesis, we have the following radical yields:

$$G_{\mathrm{CH_3}} = \alpha \cdot K_{\mathrm{CH_4}} \cdot \lambda_{\mathrm{CH_4}} \cdot [M];$$

$$G_{\mathrm{CH_2}} = \beta \cdot K_{\mathrm{CH_4}} \cdot \lambda_{\mathrm{CH_4}} \cdot [M];$$

$$G_{\mathrm{CH}} = \gamma \cdot K_{\mathrm{CH_4}} \cdot \lambda_{\mathrm{CH_4}} \cdot [M];$$

$$G_{\mathrm{H}} = (\alpha + 3\gamma) K_{\mathrm{CH_4}} \cdot \lambda_{\mathrm{CH_4}} \cdot [M];$$

$$G_{\mathrm{H_2}} = \beta \cdot K_{\mathrm{CH_4}} \cdot \lambda_{\mathrm{CH_4}} \cdot [M];$$

$$G_{\mathrm{O}} = K_{\mathrm{O_2}} \cdot \lambda_{\mathrm{O_2}} \cdot [M]$$

Eq. (1) presents a mass balance of radicals. The first term on the right hand side indicates the production term and the second term represents the formation or consumption of radicals via reactions. Eq. (2) represents the general scheme for secondary radicals during corona processing. The G value or the radical yield can then be evaluated according to:

$$G'(\text{molecules/100 eV}) = 9.649\text{e}-6 \cdot G_\mathrm{R} \cdot V_\mathrm{R} \cdot t_\mathrm{res} \tag{3}$$

where V is the volume of reactor (m^3), t_res the residence time in reactor (s) and the conversion factor, 1 eV = 1.6e−19 J, 1 mol = 6.023e23 molecules.

The dissociation constants $K_{\mathrm{CH_4}}$ and $K_{\mathrm{O_2}}$ are functions of the experimental conditions, viz. temperature, energy input and gas composition [10]. This can be obtained by numerical data fitting procedure with experimental results as done in other works [4,8] for a particular temperature and gas composition. However, the ratio of the dissociated fragments (α:β:γ) is a function of the electron energy which is similar for the case of a DBD. In a mixture of CH_4 and electron attaching gases such as CO_2, this ratio was determined to be 0.0645:0.90:0.032 (1.0e−3:1.4e−2:5.0e−4) [8,9]. Thus, in the above equation, $\alpha = 0.0645$, $\beta = 0.90$, $\gamma = 0.032$.

3.2.1. Estimation of K_{CH_4}

For a correct estimation of $K_{\mathrm{CH_4}}$ based on the present approach and for the present experimental conditions, the following factors need to be considered:

(a) the influence of joule heating needs to be minimized;
(b) radical chain reactions resulting from O_2 needs to be avoided or minimized.

Hence experiments were carried out to obtain CH_4 conversion in low O_2 concentration (CH_4:N_2:O_2 = 90:8:2) at temperature of 130 °C and power input of 2.5 W. The observed CH_4 conversion was about 1% (0.88%). Data fitting was performed by the method of least squares in order to obtain similar CH_4 conversion, as observed experimentally. The rate constant or the value of $K_{\mathrm{CH_4}}$ was calculated to be 8e−4 s^{-1} J^{-1}.

Similar procedure could not be used for obtaining the rate constant for O_2 dissociation, as in the absence of termination reactions from CH_4, most of the produced O radicals lead to O_3 formation.

$$\mathrm{e} + \mathrm{O_2} \rightarrow \mathrm{O} + \mathrm{O} + \mathrm{e}; \qquad \mathrm{O_2} + \mathrm{M} + \mathrm{e} \rightarrow \mathrm{O_3} + \mathrm{M}$$

This mechanism is not relevant in the partial oxidation scheme and therefore not included in the reactions. Hence the dissociation constant for O_2 was obtained from experiments in stoichiometric mixture of CH_4/O_2 (2:1).

3.2.2. Estimation of K_{O_2}

Using similar procedure as explained in the preceding section, the value of $K_{\mathrm{O_2}}$ was obtained to be 3e−3 s^{-1} J^{-1}. CH_4 conversion of 2.3% was realized at temperature of 130 °C with a power input of 2.5 W (about 81 kJ/mol CH_4) in a gas composition of CH_4 and O_2 (2:1). The resulting radical yields, at the

Table 1
Radical yields computed at the experimental conditions

G_{CH_3}	0.1379 mol/100 eV	G_H	0.348 mol/100 eV
G_{CH_2}	1.9242 mol/100 eV	G_{H_2}	1.924 mol/100 eV
G_{CH}	0.0648 mol/100 eV	G_O	3.8265 mol/100 eV

conditions of the experiment, can now be computed as indicated in Table 1.

The product distribution compared with the experimental results is as indicated in Fig. 4. As can be seen from Fig. 4, the calculated results do agree with the experimental results for the case of H_2, CO, CO_2. Formation of C_2 species, however could not be well explained. Terminations of the produced CH_2, CH_3 species are probably the direct pathways for C_2 formation. The most likely occurrence of such interaction is in the local discharge volumes where the condition of the uniform mixing or well mixed situation is not valid. Nevertheless, C_2 production, viz. C_2H_4, does not contribute substantially to the final product distribution. Hence, the obtained parameters can now be used for studying the chemical pathways and the significant reactions that can influence the product composition at a particular temperature.

3.2.3. Calculation at higher power input

For verification of the obtained parameters, the calculated results are compared with experimental results of Pietruszka and Heintze [6], related to gas phase CH_4 conversion in an empty DBD at 200 °C at various CH_4/O_2 ratios. Various energy definitions have been used to characterize conversion or removal of compounds in non-thermal plasma condition. For the case of CH_4 conversion, the results in the present investigation are represented as kJ/mol CH_4. Experimental data from the results of Pietruszka and Heintze [6] are re-plotted as indicated in Fig. 5. The calculated results do agree with the experimental results for the case of low power consumption (<1000 kJ/mol CH_4). However, for the case of high energy input, the conversion of the input electrical energy into thermal energy becomes significant and induces additional conversion. From energy efficiency point of view, chemical conversion resulting from thermal energy derived from electrical source at lower temperature is not desirable. Furthermore, the objective of the present paper is to investigate the plasma initiated reactions; therefore thermal reactions are not accounted for. From Fig. 5, it is quite evident that the calculated parameters and the proposed kinetic reaction scheme is adequate enough to describe the plasma assisted partial oxidation process.

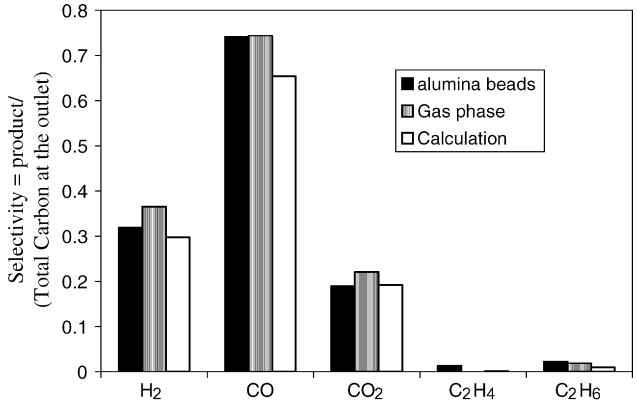

Fig. 4. Comparison of calculated and experimental results.

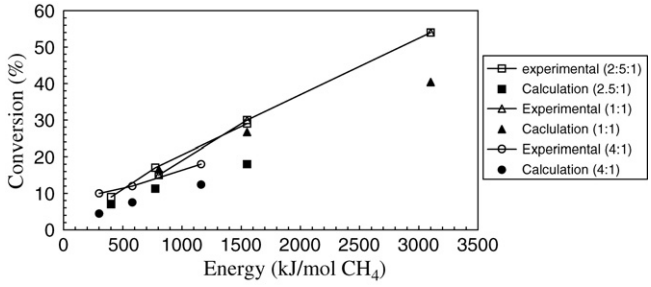

Fig. 5. Comparison of calculated and experimental results [6] at various energy input (the value in parenthesis indicate the CH_4/O_2 ratio).

3.2.4. Sensitivity analysis

One of the objectives of partial oxidation process is to obtain synthesis gas. Non-thermal plasma is used in order to facilitate reactions at lower temperature. However, as seen from the above experimental results, the selectivity for H_2 is low (<30%). A sensitivity analysis is attempted in order to determine its oxidation pathways. The above developed kinetic scheme serves as a basis for identifying the pathways which lead to increase or decrease of selectivity to H_2 and CO. A linear sensitivity analysis could be used to identify these pathways [4]. Here each reaction rate constant is increased by a factor of 10 (results are included when rate constants are changed by a factor 10) and its influence on H_2 and CO selectivity is analyzed. The present approach aims not to influence the radical production terms by the gas discharge itself, since these were estimated from experimental results. The results of the investigation is represented by a parameter S, defined as:

$$S_j = \left(\frac{Y_j - Y_{j0}}{Y_{j0}}\right) \times 100 \quad (4)$$

where Y_j is the selectivity when the rate constant of the reaction "j" is increased by a factor 10 and Y_{j0} is the actual selectivity (when rate constant is not altered).

Thus, a positive value for S, would indicate an increase in corresponding selectivity, and vice versa. The results of the analysis are presented in Fig. 6(a and b) for the case of H_2 and CO, respectively. The following observations can be made from the results of the sensitivity analysis:

(1) As per the mechanism proposed in Fig. 3, one of the pathways for H_2 production results from CH_2O/CH_3OH oxidation. Formation of CH_3O and its subsequent reactions lead to a decrease in H_2 production. From the reactions listed in Appendix A, it can be inferred that one of the pathways for CH_3O formation is from the termination of the liquid products such as CH_2O and CH_3OH. Hence, a high density of O/H radicals should favor H_2 production.

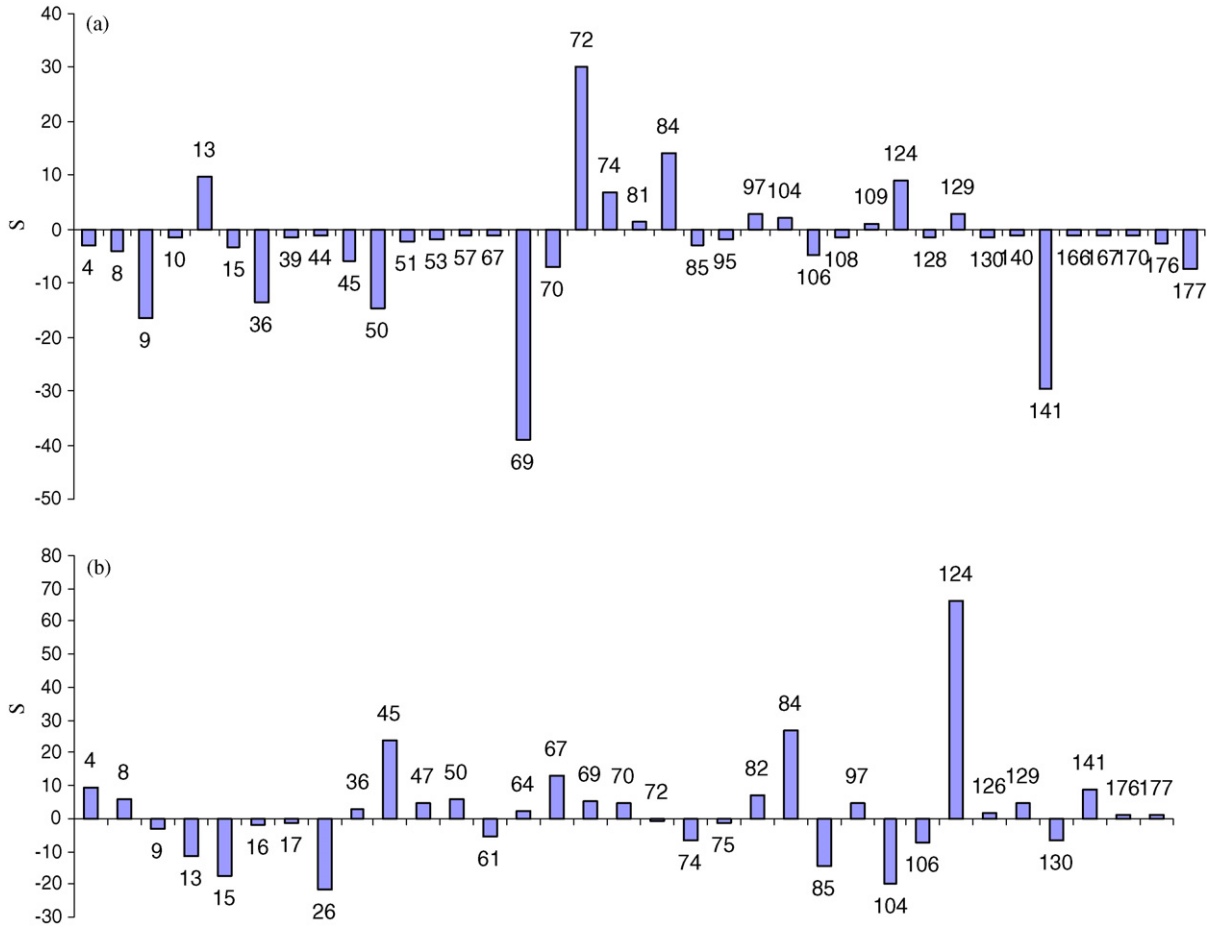

Fig. 6. Sensitivity analysis for: (a) CO and (b) H_2.

(2) A high concentration of OH radicals leads to a decrease in the H_2 selectivity. This can be a direct result of third body reaction of H and OH to produce H_2O.
(3) Although reaction no. 84 seems to influence H_2 production significantly, from the mechanistic point of view, it cannot be clearly explained. Since the major contribution of this reaction is for regeneration of CH_4 and O_2, which re-initiates the partial oxidation process.
(4) A general conclusion related to factors affecting decrease in CO production is the termination of CH_3 radicals. This is quite evident from the sensitivity exhibited towards reactions 36, 69, 141. An increased production of CH_3 (reaction 69) is accompanied by its termination to CH_4 via reaction 69 and further termination via reaction 141 to C_3 formation.

Overall, the mechanism proposed in Fig. 3, is valid for predicting/explaining the product spectrum for the case of partial oxidation process at the experimental conditions. In both cases (Fig. 6(a and b)), the pathways for H_2 and CO formation is via the oxidation of the intermediate C_1 oxygenates. Recent studies [11] with in situ FTIR spectroscopy, during non-thermal plasma assisted methane oxidative conversion, have as well indicated the presence of oxygenates as an intermediate product at stoichiometric ($CH_4/O_2 = 1.8–2$) compositions. However, the termination reactions for both cases (Fig. 6(a and b)) differ considerably. For the case of H_2 formation, the termination of liquid products to CH_3O limits H_2 selectivity, while for CO, the termination of the dissociated fragments CH_3, CH_2, etc., acts as a limiting reaction.

4. Combined partial oxidation and steam reforming

An alternative method to increase H_2 production is by combined partial oxidation and steam reforming. In the conventional thermal or catalytic process, the intention to combine these two distinctive approaches would be to utilize the heat liberated from the partial oxidation/combustion of methane for the endothermic reforming process. In a non-thermal plasma assisted process, the objective is to split water molecules either by energetic electron molecule collisions processes or by the radical reactions initiated by the methane partial oxidation process. However, experiments in the presence of steam did not result in significant change in the product distribution or in the conversion of CH_4 at similar experimental conditions ($T < 200\,^{\circ}C$, $E < 200$ kJ/mol CH_4), except for the production of liquid phase products such as CH_2O and CH_3OH. A product distribution in presence of steam during partial oxidation of CH_4 is indicated in Fig. 7. The results

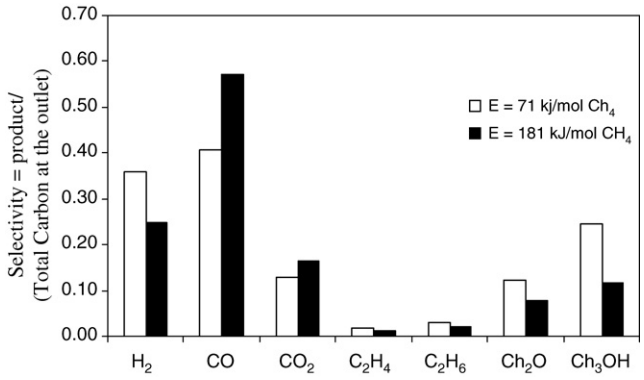

Fig. 7. Product distribution seen at different energy input for the case of $CH_4/O_2 = 2$.

indicate a higher selectivity towards formation of oxygenates at lower energy density ($E < 100$ kJ/mol CH_4). With an increase in energy input, the selectivity towards oxygenates decreases. In order to elucidate the mechanism of formation of liquid oxygenates, an in situ investigation is needed. Isotopes have been frequently employed in mechanistic investigations in order to trace the path of reactions. In this study, D_2O is used in order to identify steam conversion pathways or the role of steam in the mixed gas system (CH_4/O_2/steam) in non-thermal plasma.

Dissociation of molecules in non-thermal plasma is related to the gas composition. As can be seen from the calculated results in the earlier section and as well as from other works [2,3,8], not only gas composition but also the nature of the gas components influence the radical production process.

For the mechanistic investigation, experiments were done for the following cases:

(a) pure steam reforming;
(b) combined partial oxidation and reforming.

D_2O was used to generate steam and the resulting product distribution was analyzed by means of GC (TCD and FID) and a mass spectrometer (QMS). The temperature was kept constant as in the earlier experiments at 130 °C and at a constant power input of 2.5 kW or 100 kJ/mol CH_4.

Fig. 8(a and b) indicates the relative contribution to H_2 formation from steam and CH_4 at various temperature (130 and 200 °C) and CH_4/O_2 ratio. D_2O was used to generate steam. H_2, HD and D_2 was particularly studied since H_2 would be one of the product formed resulting from steam conversion. An obvious conclusion from the observed results is that in presence of O_2, steam conversion is almost negligible. Results indicate that in presence of O_2, dissociation of water molecules by plasma is almost negligible. Perhaps the only contribution is to act as a carrier for the intermediates formed during the conversion process. In other words, it acts as a quenching media for the partial oxidation process. The problem then is not related to reaction kinetics, but mass transfer of the produced oxygenates in order to quench the reaction. This can perhaps explain the observed liquid products observed during the conversion

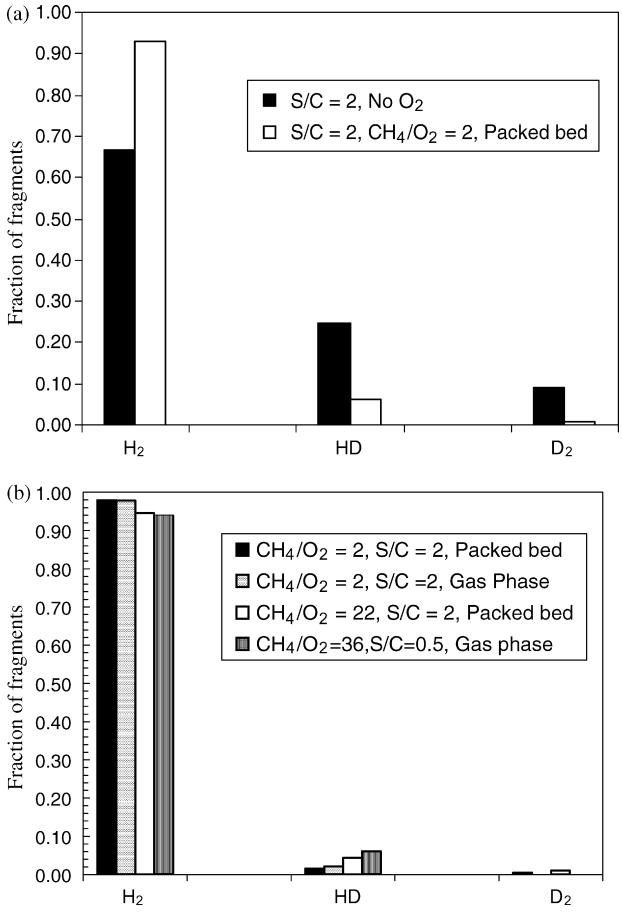

Fig. 8. Relative contribution to H_2 formation from steam and CH_4 at varying temperature: (a) $T = 130$ °C, $E = 71$ kJ/mol CH_4 and (b) $T = 200$ °C, $E = 71$ kJ/mol CH_4.

process (Fig. 7). A further analysis of the results in Fig. 7 would also indicate the confirmation of the reaction pathways indicated in Fig. 3. At lower energy inputs, liquid oxygenate production is higher, which further dissociates as energy input is increased. Thus, quenching the reaction can lead to higher oxygenates production. Similar results related to liquid oxygenates production has been reported [12], where, instead of steam, cooled electrode walls and micro gaps have been used in order to quench the reaction, and therefore avoid further gas phase oxidation.

Based on the above analysis, further work would focus on incorporating the "right" catalytic surface in order to control the product formation. From the available results, with the present configuration, only stable molecules or intermediates formed during the course of gas phase reaction have sufficient lifetime to interact/react at the surface. Alternative reactor design or electrode design can be incorporated in order to generate plasma on the surface so as to decrease mass transfer limitation [3]. This will be part of the further work.

5. Summary and conclusion

The following observations could be drawn from the analysis presented in the present paper:

(1) Plasma assisted CH_4 partial oxidation process at a ratio of 2–4 proceeds mainly via oxygenate formation.
(2) Excess oxidation of H_2 is one of the limiting reactions for increasing H_2 production/selectivity at the experimental conditions. For the case of CO, the termination reaction of the dissociated fragments acts as a limiting reaction.
(3) In the presence of O_2, steam conversion is almost negligible at the experimental conditions. The main role is to quench the reaction or otherwise to separate the stable intermediates formed during the course of the reaction.

Acknowledgements

One of the authors (S.A. Nair) wishes to acknowledge JSPS (Japan Society for Promotion of Science) for their financial support. The authors also wish to thank Dr. K. Yan (Faculty of Electrical Engineering, Eindhoven University of Technology, The Netherlands) for the fruitful discussions and valuable suggestions.

Appendix A

Reactions and the rate constants (rate constants are obtained from: http://kinetics.nist.gov/chemistry)

Number	Reaction	Rate coefficient, $AT^n \exp(-E/RT)$		
		A (mol cm^3 s)	n (T in K)	E (cal/mol)
1	$O + O + M \rightarrow O_2 + M$	1.89001E+13	0	−1,790
2	$O + H + M \rightarrow OH + M$	4.71334E+18	−1	0
3	$O + H_2 \rightarrow H + OH$	51311.40194	2.67	6,280
4	$O + HO_2 \rightarrow OH + O_2$	3.25242E+13	0	0
5	$O + H_2O_2 \rightarrow OH + HO_2$	9630940.048	2	3,970
6	$O + CH \rightarrow H + CO$	3.96916E+13	0	0
7	$O + CH_2 \rightarrow H + HCO$	3.01752E+13	0	0
8	$O + CH_3 \rightarrow H + CH_2O$	8.4322E+13	0	0
9	$O + CH_4 \rightarrow OH + CH_3$	692084013.4	1.56	8,490
10	$O + CO + M \rightarrow CO_2 + M$	6.16701E+14	0	3,000
11	$O + HCO \rightarrow OH + CO$	3.0115E+13	0	0
12	$O + HCO \rightarrow H + CO_2$	3.0115E+13	0	0
13	$O + CH_2O \rightarrow OH + HCO$	4.16802E+11	0.57	2,760
14	$O + CH_2OH \rightarrow OH + CH_2O$	6.023E+12	0	0
15	$O + CH_3O \rightarrow OH + CH_2O$	6.023E+12	0	0
16	$O + CH_3OH \rightarrow OH + CH_2OH$	3.43913E+13	0	5,460
17	$O + CH_3OH \rightarrow OH + CH_3O$	9.99818E+12	0	4,690
18	$O + C_2H \rightarrow CH + CO$	1.01789E+13	0	0
19	$O + C_2H_2 \rightarrow H + HCCO$	9.0345E+12	0	4,530
20	$O + C_2H_2 \rightarrow CO + CH_2$	409785428.6	1.5	1,700
21	$O + C_2H_4 \rightarrow CH_3 + HCO$	132089687.6	1.55	430
22	$O + C_2H_5 \rightarrow CH_3 + CH_2O$	1.60814E+13	0	0
23	$O + C_2H_6 \rightarrow OH + C_2H_5$	999876445.7	1.5	5,800
24	$O_2 + CO \rightarrow O + CO_2$	2.52966E+12	0	47,690
25	$O_2 + CH_2O \rightarrow HO_2 + HCO$	2.04782E+13	0	38,950
26	$H + O_2 + M \rightarrow HO_2 + M$	1.41143E+18	−0.8	0
27	$H + O_2 \rightarrow O + OH$	1.98759E+14	0	16,810
28	$H + H + M \rightarrow H_2 + M$	5.43436E+18	−1.3	0
29	$H + OH + M \rightarrow H_2O + M$	8.34369E+21	−2	0
30	$H + HO_2 \rightarrow O + H_2O$	3.0115E+13	0	1,720
31	$H + HO_2 \rightarrow O_2 + H_2$	6.6253E+13	0	2,130
32	$H + HO_2 \rightarrow OH + OH$	1.69246E+14	0	870
33	$H + H_2O_2 \rightarrow HO_2 + H_2$	4.8184E+13	0	7,950
34	$H + H_2O_2 \rightarrow OH + H_2O$	2.4092E+13	0	3,970
35	$H + CH_2(+M) \rightarrow CH_3(+M)$	1.04E+26	−2.76	1,600
36	$H + CH_3(+M) \rightarrow CH_4(+M)$	3.103E+24	−1.8	0
37	$H + CH_4 \rightarrow CH_3 + H_2$	13268.82987	3	8,030
38	$H + HCO(+M) \rightarrow CH_2O(+M)$	2.65162E+24	−2.57	430
39	$H + HCO \rightarrow H_2 + CO$	1.21062E+14	0	0
40	$H + CH_2O(+M) \rightarrow CH_2OH(+M)$	12588070000	0	1,190
41	$H + CH_2O(+M) \rightarrow CH_3O(+M)$	2.2E+30	−4.8	5,560
42	$H + CH_2O \rightarrow HCO + H_2$	22802215455	1.05	3,280
43	$H + CH_2OH \rightarrow H_2 + CH_2O$	6.023E+12	0	0
44	$H + CH_2OH \rightarrow OH + CH_3$	9.6368E+13	0	0
45	$H + CH_3O(+M) \rightarrow CH_3OH(+M)$	4.66E+41	−7.44	14,080
46	$H + CH_3O \rightarrow H + CH_2OH$	41500000	1.6	1,924
47	$H + CH_3O \rightarrow H_2 + CH_2O$	1.98759E+13	0	0
48	$H + CH_3O \rightarrow OH + CH_3$	1.5E+12	0.5	−110

Appendix A (*Continued*)

Number	Reaction	Rate coefficient, $AT^n \exp(-E/RT)$		
		A (mol cm^3 s)	n (T in K)	E (cal/mol)
49	$H + CH_3OH \rightarrow CH_2OH + H_2$	16413292.19	2	4,510
50	$H + CH_3OH \rightarrow CH_3O + H_2$	18062558548	3.4	7,230
51	$H + C_2H(+M) \rightarrow C_2H_2(+M)$	1.81292E+14	0	0
52	$H + C_2H_2(+M) \rightarrow C_2H_3(+M)$	5.499E+12	0	2,420
53	$H + C_2H_3(+M) \rightarrow C_2H_4(+M)$	5.36047E+14	0	980
54	$H + C_2H_3 \rightarrow H_2 + C_2H_2$	1.99964E+13	0	0
55	$H + C_2H_4(+M) \rightarrow C_2H_5(+M)$	841589685.2	1.49	990
56	$H + C_2H_4 \rightarrow C_2H_3 + H_2$	1324663.916	2.53	12,240
57	$H + C_2H_5(+M) \rightarrow C_2H_6(+M)$	9.99818E+13	0	0
58	$H + C_2H_5 \rightarrow H_2 + C_2H_4$	1.81292E+12	0	0
59	$H + C_2H_6 \rightarrow C_2H_5 + H_2$	553.7391495	3.5	5,170
60	$H_2 + CO(+M) \rightarrow CH_2O(+M)$	5.07E+27	−3.42	84,350
61	$OH + H_2 \rightarrow H + H_2O$	6375411.018	2	2,960
62	$OH + OH(+M) \rightarrow H_2O_2(+M)$	2.89214E+17	−0.76	0
63	$OH + OH \rightarrow O + H_2O$	1502070325	1.14	100
64	$OH + HO_2 \rightarrow O_2 + H_2O$	2.89104E+13	0	−500
65	$OH + H_2O_2 \rightarrow HO_2 + H_2O$	7.8299E+12	0	1,330
66	$OH + CH_2 \rightarrow H + CH_2O$	1.81292E+13	0	0
67	$OH + CH_3(+M) \rightarrow CH_3OH(+M)$	6.023E+13	0	0
68	$OH + CH_3 \rightarrow CH_2 + H_2O$	1110.667063	3	2,780
69	$OH + CH_4 \rightarrow CH_3 + H_2O$	15667391.41	1.83	2,780
70	$OH + CO \rightarrow H + CO_2$	6322403.755	1.5	500
71	$OH + HCO \rightarrow H_2O + CO$	3.0115E+13	0	0
72	$OH + CH_2O \rightarrow HCO + H_2O$	3428457832	1.18	−450
73	$OH + CH_2OH \rightarrow H_2O + CH_2O$	2.4092E+13	0	0
74	$OH + CH_3O \rightarrow H_2O + CH_2O$	1.81292E+13	0	0
75	$OH + CH_3OH \rightarrow CH_2OH + H_2O$	24466.15745	2.8	420
76	$OH + CH_3OH \rightarrow CH_3O + H_2O$	17.31674968	3.4	−1,140
77	$OH + C_2H_2 \rightarrow C_2H + H_2O$	14512.77627	2.68	12,040
78	$OH + C_2H_2 \rightarrow CH_3 + CO$	0.000484214	4	−2,010
79	$OH + C_2H_3 \rightarrow H_2O + C_2H_2$	3.0115E+13	0	0
80	$OH + C_2H_4 \rightarrow C_2H_3 + H_2O$	15697.34578	2.75	4,170
81	$OH + C_2H_6 \rightarrow C_2H_5 + H_2O$	8850965298	1.04	1,810
82	$HO_2 + HO_2 \rightarrow O_2 + H_2O_2$	1.81292E+12	0	0
83	$HO_2 + CH_2 \rightarrow OH + CH_2O$	2E+13	0	0
84	$HO_2 + CH_3 \rightarrow O_2 + CH_4$	3.60778E+12	0	0
85	$HO_2 + CH_3 \rightarrow OH + CH_3O$	1.98759E+13	0	0
86	$HO_2 + CO \rightarrow OH + CO_2$	1.51177E+14	0	23,650
87	$HO_2 + CH_2O \rightarrow HCO + H_2O_2$	1.98759E+12	0	11,660
88	$CH + O_2 \rightarrow O + HCO$	9.99818E+12	0	0
89	$CH + H_2 \rightarrow H + CH_2$	332068336	1.79	1,670
90	$CH + H_2O \rightarrow CH_2OH$	5.7098E+12	0	760
91	$CH + CH_2 \rightarrow H + C_2H_2$	4E+13	0	0
92	$CH + CH_3 \rightarrow H + C_2H_3$	3E+13	0	0
93	$CH + CH_4 \rightarrow H + C_2H_4$	1.50575E+12	0	0
94	$CH + CO(+M) \rightarrow HCCO(+M)$	9.93999E+12	−0.4	0
95	$CH + CO_2 \rightarrow HCO + CO$	1.9E+14	0	0
96	$CH + HCCO \rightarrow CO + C_2H_2$	5E+13	0	0
97	$CH_2 + O_2 \rightarrow H_2O + CO$	2.4092E+11	0	0
98	$CH_2 + H_2 \rightarrow H + CH_3$	3011500000	0	0
99	$CH_2 + CH_2 \rightarrow H_2 + C_2H_2$	3.19219E+13	0	0
100	$CH_2 + CH_3 \rightarrow H + C_2H_4$	4.2161E+13	0	0
101	$CH_2 + CH_4 \rightarrow CH_3 + CH_3$	181292.3	0	0
102	$CH_2 + HCCO \rightarrow C_2H_3 + CO$	3E+13	0	0
103	$CH_3 + O_2 \rightarrow O + CH_3O$	7.18226E+11	0.39	27,420
104	$CH_3 + O_2 \rightarrow OH + CH_2O$	3.403E+11	0	8,940
105	$CH_3 + H_2O_2 \rightarrow HO_2 + CH_4$	12106230000	0	600
106	$CH_3 + CH_3(+M) \rightarrow C_2H_6(+M)$	1.01108E+15	−0.64	0
107	$CH_3 + CH_3 \rightarrow H + C_2H_5$	4.97444E+12	0.1	10,610
108	$CH_3 + HCO \rightarrow CH_4 + CO$	1.21062E+14	0	0
109	$CH_3 + CH_2O \rightarrow HCO + CH_4$	5542.671115	2.81	5,860
110	$CH_3 + CH_3OH \rightarrow CH_2OH + CH_4$	31.90031185	3.2	7,170

Appendix A (*Continued*)

Number	Reaction	Rate coefficient, $AT^n \exp(-E/RT)$		
		A (mol cm^3 s)	n (T in K)	E (cal/mol)
111	$CH_3 + CH_3OH \rightarrow CH_3O + CH_4$	14.41984085	3.1	6,940
112	$CH_3 + C_2H_4 \rightarrow C_2H_3 + CH_4$	6.623878207	3.7	9,500
113	$CH_3 + C_2H_6 \rightarrow C_2H_5 + CH_4$	0.54913193	4	8,290
114	$HCO + M \rightarrow H + CO + M$	1.87E+17	−1	17,000
115	$HCO + O_2 \rightarrow HO_2 + CO$	5.11955E+13	0	1,690
116	$CH_2OH + O_2 \rightarrow HO_2 + CH_2O$	1.21062E+12	0	0
117	$CH_3O + O_2 \rightarrow HO_2 + CH_2O$	66253000000	0	2,600
118	$C_2H + O_2 \rightarrow HCO + CO$	2.41522E+12	0	0
119	$C_2H + H_2 \rightarrow H + C_2H_2$	1.12028E+13	0	2,860
120	$C_2H_3 + O_2 \rightarrow HCO + CH_2O$	4.56965E+16	−1.39	1,010
121	$C_2H_5 + O_2 \rightarrow HO_2 + C_2H_4$	8.4322E+11	0	3,880
122	$HCCO + O_2 \rightarrow OH + CO + CO$	3.2E+12	0	854
123	$HCCO + HCCO \rightarrow CO + CO + C_2H_2$	1E+13	0	0
124	$O + CH_3 \rightarrow H + H_2 + CO$	1.17449E+13	0	−400
125	$O + C_2H_4 \rightarrow C_2H_3 + OH$	15062998.74	1.91	3,740
126	$OH + HO_2 \rightarrow O_2 + H_2O$	1.44486E+16	−1	0
127	$OH + CH_3 \rightarrow H_2 + CH_2O$	3.19483E+12	−0.53	10,810
128	$CH + H_2(+M) \rightarrow CH_3(+M)$	5.15082E+13	0.15	0
129	$O_2 + CH_2 \rightarrow CO + H_2O$	2.4092E+11	0	0
130	$CH_2 + O_2 \rightarrow O + CH_2O$	2.4E+12	0	1,500
131	$CH_2 + CH_2 \rightarrow H + H + C_2H_2$	1.99964E+14	0	10,989
132	$C_2H_3 + O_2 \rightarrow HO_2 + C_2H_2$	1.21062E+11	0	0
133	$CH_3 + C_2H_5(+M) \rightarrow C_3H_8(+M)$	4.88674E+14	−0.5	0
134	$O + C_3H_8 \rightarrow OH + C_3H_7$	3701868.935	2.4	5,500
135	$H + C_3H_8 \rightarrow C_3H_7 + H_2$	1323256.146	2.54	6,760
136	$OH + C_3H_8 \rightarrow C_3H_7 + H_2O$	5391969.956	2	450
137	$C_3H_7 + H_2O_2 \rightarrow HO_2 + C_3H_8$	18664.81867	2.11	2,560
138	$CH_3 + C_3H_8 \rightarrow C_3H_7 + CH_4$	0.903128142	3.65	7,150
139	$CH_3 + C_2H_4(+M) \rightarrow C_3H_7(+M)$	3.31265E+11	0	7,710
140	$O + C_3H_7 \rightarrow C_2H_5 + CH_2O$	9.64E+13	0	0
141	$H + C_3H_7(+M) \rightarrow C_3H_8(+M)$	4.42E+61	−13.54	11,357
142	$H + C_3H_7 \rightarrow CH_3 + C_2H_5$	4060000	2.2	890
143	$OH + C_3H_7 \rightarrow C_2H_5 + CH_2OH$	2.41E+13	0	0
144	$HO_2 + C_3H_7 \rightarrow O_2 + C_3H_8$	25500000000	0.3	−943
145	$HO_2 + C_3H_7 \rightarrow OH + C_2H_5 + CH_2O$	2.41E+13	0	0
146	$CH_3 + C_3H_7 \rightarrow C_2H_5 + C_2H_5$	1.93E+13	−0.3	0
147	$H_2O_2 \rightarrow OH + OH$	1.2942E+33	−4.86	53,260
148	$H_2O + O \rightarrow OH + OH$	4573426805	1.3	17,098
149	$CH_3 + H \rightarrow CH_2 + H_2$	6.08323E+13	0	15,100
150	$CH_3 + O \rightarrow CH_3O$	7.95777E+15	−2.12	620
151	$HO_2 + H_2O_2 \rightarrow OH + H_2O + O_2$	3.0115E+13	0	
152	$HCO + H_2O_2 \rightarrow CH_2O + HO_2$	1.01789E+11	0	
153	$HCO + HO_2 \rightarrow OH + H + CO_2$	3.0115E+13	0	
154	$HO_2 + H_2O \rightarrow OH + H_2O_2$	2.8007E+13	0	
155	$HCO + H_2O \rightarrow CH_2O + OH$	23500590631	1.35	
156	$HCO + HCO \rightarrow CH_2O + CO$	1.8069E+13	0	
157	$O_2 + H_2O_2 \rightarrow HO_2 + HO_2$	5.4207E+13	0	
158	$O_2 + HCO \rightarrow CO + HO_2$	5.11955E+13	0	
159	$CH_2O \rightarrow CO + H_2$	1.51E+14	0	101,000
160	$C_2H_6 + HO_2 \rightarrow H_2O_2 + C_2H_5$	2.95127E+11	0	14,940
161	$C_2H_6 + HCO \rightarrow CH_2O + C_2H_5$	46894.3917	2.72	18,240
162	$C_2H_6 + O_2 \rightarrow HO_2 + C_2H_5$	4.04143E+13	0	50,870
163	$CH_4 + O_2 \rightarrow CH_3 + HO_2$	4.04143E+13	0	56,830
164	$CH_2O + C_2H_5 \rightarrow C_2H_6 + HCO$	5502.36078	2.81	5,860
165	$C_2H_4 + O_2 \rightarrow C_2H_3 + HO_2$	4.22212E+13	0	57,630
166	$O + C_2H_3 \rightarrow CH_2CO + H$	9.6368E+13	0	0
167	$O + HCCO \rightarrow H + 2CO$	9.6368E+13	0	0
168	$O + CH_2CO \rightarrow OH + HCCO$	1E+13	0	8,000
169	$O + CH_2CO \rightarrow CH_2 + CO_2$	1.75E+12	0	1,350
170	$H + CH_2OH \rightarrow CH_3OH$	6E+32	−4.8	3,300
171	$H + CH_2CO \rightarrow HCCO + H_2$	5E+13	0	8,000
172	$H + CH_2CO \rightarrow CH_3 + CO$	1.13E+13	0	3,428

Appendix A (*Continued*)

Number	Reaction	Rate coefficient, $AT^n \exp(-E/RT)$		
		A (mol cm^3 s)	n (T in K)	E (cal/mol)
173	$H + HCCOH \rightarrow H + CH_2CO$	1E+13	0	0
174	$OH + C_2H \rightarrow H + HCCO$	2E+13	0	0
175	$OH + C_2H_2 \rightarrow H + CH_2CO$	0.000219885	4.5	−1,000
176	$CH + CH_2O \rightarrow H + CH_2CO$	9.46E+13	0	−515
177	$CH_2 + CO \rightarrow CH_2CO$	2.69E+33	−5	7,095
178	$C_2H_4 \rightarrow H_2 + C_2H_2$	7E+50	−9.31	99,860
179	$OH + C_2H \rightarrow CO + CH_2$	1.8069E+13	0	
180	$OH + C_2H \rightarrow O + C_2H_2$	1.8069E+13	0	

References

[1] Q. Zhu, X. Zhao, Y. Deng, Advances in the partial oxidation of methane to synthesis gas, J. Nat. Gas Chem. 13 (2004) 191–203.

[2] K. Yan, Corona plasma generation, PhD Thesis, Eindhoven University of Technology, Eindhoven, 2001.

[3] S.A. Nair, Corona plasma for tar removal, PhD Thesis, Eindhoven University of Technology, Eindhoven, 2004.

[4] S.A. Nair, A.J.M. Pemen, K. Yan, E.J.M. van Heesch, K.J. Ptasinski, A.A.H. Drinkenburg, Tar removal from biomass derived fuel gas by pulsed corona discharges—a chemical kinetic study, Ind. Eng. Chem. Res. 43 (2004) 1649–1658.

[5] K. Supat, S. Chavadej, L.L. Lobban, R.G. Mallinson, Combined steam reforming and partial oxidation of methane to synthesis gas under electrical discharge, Ind. Eng. Chem. Res. 42 (2003) 1654–1661.

[6] B. Pietruszka, M. Heintze, Methane conversion at low temperature: the combined application of catalysis and non-equilibrium plasma, Catal. Today 90 (2004) 151–158.

[7] B. Eliasson, F.G. Simon, W. Egli, Hydrogenation of CO_2 in a silent discharge, Non-Therm. Plasma Tech. Pollut. Control Part B (1992) 321–337.

[8] M. Kraus, Catalytic CO_2 reforming of methane in a dielectric barrier discharge, PhD Thesis, Swiss Federal Institute of Technology, Zurich, 2001.

[9] M. Kraus, W. Egli, K. Haffner, B. Eliasson, U. Kogelschatz, A. Wokaun, Investigation of mechanistic aspects of the catalytic CO_2 reforming of methane in a dielectric-barrier discharge using optical emission spectroscopy and kinetic modeling, Phys. Chem. Chem. Phys. 4 (4) (2002) 668–675.

[10] S.A. Nair, K. Yan, A.J.M. Pemen, E.J.M. van Heesch, K.J. Ptasinski, A.A.H. Drinkenburg, Tar removal from biomass derived fuel gas by pulsed corona discharges—a chemical kinetic study II, Ind. Eng. Chem. Res. 44 (2005) 1734–1741.

[11] S.A. Nair, T. Nozaki, K. Okazaki, In situ FTIR study of non thermal plasma assisted methane oxidative conversion, Ind. Eng. Chem. Res., in press.

[12] D.W. Larkin, L. Zhou, L.L. Lobban, R.G. Mallinson, Product selectivity control and organic oxygenate pathways from partial oxidation of methane in a silent electric discharge reactor, Ind. Eng. Chem. Res. 40 (2001) 5496–5506.